Microbiomes without boundaries: cystic fibrosis 'pulmotype' classifications are dependent on algorithm choice and database size, and indicate continuous variation.

Conan Y. Zhao[1,2,3]*, Ryan Lowhorn[1,2]*, Haojun Song[1,2,4], Jinyoung Eum[1,2,5], & Sam P. Brown[1,2]#

1. School of Biological Sciences, College of Sciences, Georgia Institute of Technology, Atlanta, GA, USA
2. Center for Microbial Dynamics and Infection, Georgia Institute of Technology, Atlanta, GA, USA
3. Alix School of Medicine, Mayo Clinic, Rochester, MN USA

*Co-first author

corresponding author (sam.brown@biology.gatech.edu)

Abstract

A common response to microbiome sample variation is to use clustering algorithms to reduce complex and variable datasets to a smaller number of 'types' (e.g. enterotypes for gut samples, or pulmotypes for lung samples). In light of recent analyses showing distinct clustering solutions to in principle similar datasets, we examine the extent to which clustering solutions are dependent on researcher choices of algorithm and dataset, using cystic fibrosis (CF) sputum microbiome data as a model system. Following a structured literature review, we identified 36 CF microbiome studies with publicly available samples and metadata. From these studies we curated a dataset of 4026 sputum microbiome samples across 1184 people with CF (pwCF), complete with matched individual metadata, using a standardized bio-informatic platform. Applying multiple clustering algorithms (DMM, k-means, PAM) to cross-sectional data we find that the optimal partitioning depends on both choice of algorithm and database size, with generally weak separation among clusters in any classification. Our longitudinal data analyses highlight substantial persistence of cluster types in time, with transitions most common among clusters that are structurally similar, reflecting an underlying continuous landscape of microbiome variation. While transitions among similar clusters are common (e.g. along gradients of *Pseudomonas aeruginosa* relative abundance), transitions are generally bi-directional, with no clear pathogen-dominated 'end point' states. Together our results highlight that clustering tools can generate arbitrary and inconsistent boundaries on a continuously varying landscape of microbiome variation.

Introduction

Microbiome samples from natural (including human) sources are often strikingly variable, even when sampled from seemingly similar locations. For example, fecal microbiome samples can vary substantially across people, even among healthy individuals(Arumugam et al., 2011). One approach to simplify this variation is to cluster individual samples into a smaller number of representative modal 'types'. This clustering approach has been extensively used in the gut microbiome literature to define 'enterotypes'(Arumugam et al., 2011, Knights et al., 2014, Costea et al., 2018), and more recently has been applied to lung microbiomes under the term 'pulmotypes', notably in the context of people with cystic fibrosis(Widder et al., 2022, Hampton et al., 2021).

Cystic fibrosis (CF) is a genetic disease affecting more than 30,000 people in the US and approximately 70,000 people globally. CF is characterized by chronic, polymicrobial infections of the respiratory tract. Culture-independent sequencing of sputum samples from people with CF (pwCF) have identified thousands of taxa including canonical CF pathogens such as *Pseudomonas aeruginosa* and taxa from commensal oral and nasopharyngeal microbiomes(Caverly et al., 2015, Widder et al., 2022, Hampton et al., 2021). While commonly observed in sputum samples, the functional role of these commensal taxa remains a topic of ongoing debate. Many observational CF studies report a positive association between commensal abundance and lung function(Coburn et al., 2015, Cuthbertson et al., 2016, Widder et al., 2022, Zhao et al., 2012, Zhao et al., 2020) consistent with a beneficial role of commensals. However, experimental *in vitro* microbiome studies show mixed results, with commensals either facilitating or inhibiting pathogen growth, depending on environmental context or species involved(Flynn et al., 2016, Varga et al., 2022). Additionally, the potential for salivary and oral

microbiome contamination during sputum expectoration adds a layer of complexity to pulmonary microbiome analyses(Goddard et al., 2012, Jorth et al., 2019), although for patients with more advanced disease this contamination likely has a limited impact(Lu et al., 2020).

To address the substantial variation across CF microbiomes, two studies have applied clustering techniques to categorize these microbiomes into distinct "pulmotypes". Hampton et al. (Hampton et al., 2021) used k-means clustering on sputum samples from 167 pwCF, identifying five distinct community types which included three dominated by *Pseudomonas*, one dominated by oral taxa, and one mixed-pathogens pulmotype that pooled together diverse cases of established CF pathogens (*Achromobacter*, *Burkholderia*, *Haemophilus*). Widder et al. (Widder et al., 2022) employed a Dirichlet Multinomial Mixture model (DMM) to classify 818 sputum samples across a cohort of 109 pwCF into eight pulmotypes, including separate clusters dominated by *Burkholderia* and *Staphylococcus* along with multiple *Pseudomonas* dominant clusters. Such classification approaches aim to reduce high-dimensional data into more manageable groupings, allowing simpler health outcome comparisons and characterizations of disease progression. Furthermore, defining 'pulmotypes' provides a rationale for the development of *in vitro* synthetic microbiomes that potentially represent clinically relevant microbiome structures(Varga et al., 2022, Jean-Pierre et al., 2023).

In light of contrasting pulmotyping methods in the literature(Widder et al., 2022, Hampton et al., 2021), critical questions arise on the robustness of the classifications, and in particular their dependence on the choice of data and algorithm. Individual studies often use relatively small sample sets and varying methodologies, which complicates cross-study comparisons. To address these challenges, we aimed to compile all publicly available CF sputum

microbiome data to evaluate whether existing clustering approaches yield consistent classifications across differing choices of algorithm and dataset size.

In this study, we integrate publicly available 16S microbiome data from over 4,000 sputum samples from more than 1,000 pwCF. Beginning with raw reads from NCBI, we applied a standardized bioinformatics pipeline to mitigate methodological discrepancies in data processing. Using this comprehensive dataset, we show that the optimal clustering scheme is highly sensitive to choices of clustering algorithm, with optimal cluster number varying from 2 to 12 on the same dataset. We further show that for some algorithms, the optimal scheme is also strongly sensitive to database size. Using both cross-sectional and longitudinal analyses, we highlight that various cluster partitions generate arbitrary boundaries on a continuously varying landscape of variation. We review the utility of cluster algorithms in light of these results, highlighting the limitations of discrete cluster assumptions given a continuously varying landscape of CF microbiome samples.

Results

A Standardized CF Microbiome Database

Using a structured search of NCBI SRA for CF lung microbiome 16S amplicon reads (see methods), we curated a database of 4026 sputum compositions across 1184 individuals with CF from 36 published studies (median 53 samples per study; 1-163 samples per individual pwCF), Table 1. Our database uses a common read processing pipeline (see methods) and represents 26 CF centers across 14 countries (Figure 1A). Given the variation in both inclusion criteria and methodological choices within each component study, we hypothesized that

methodological and regional differences will result in compositional differences among studies. Consistent with this hypothesis, we see significant differences in composition in multiple pairwise study comparisons (Figure 1B, Analysis of Similarity ANOSIM R $p < 0.05$ Bonferroni corrected), yet effect sizes rarely approached our threshold for a substantial effect (ANOSIM R > 0.4(Roberts et al., 2008)).

Table 1. NCBI Bioproject numbers and linked references, where available. Data available via https://www.ncbi.nlm.nih.gov/bioproject.

PRJEB1219(Tunney et al., 2013)	PRJNA437613(Hahn et al., 2019)
PRJEB27573(Quinn et al., 2018)	PRJNA445243(Keravec et al., 2019)
PRJEB27575(Quinn et al., 2018)	PRJNA480715(Grahl et al., 2018)
PRJEB28175(Quinn et al., 2019)	PRJNA488913(Terranova et al., 2018)
PRJEB30646(Cuthbertson et al., 2020)	PRJNA504944(Tueffers et al., 2019)
PRJEB31332(Garcia-Nuñez et al., 2020)	PRJNA520924(Caverly et al., 2019)
PRJEB34389(Ronchetti et al., 2018)	PRJNA544655(Voronina et al., 2020)
PRJEB36034(Raghuvanshi et al., 2020)	PRJNA544933(Voronina et al., 2020)
PRJEB38277(Weiser et al., 2021)	PRJNA548026(Maestrali et al., 2020)
PRJEB8060(Kramer et al., 2015)	PRJNA594304(Caverly et al., 2021)
PRJNA207555(Price et al., 2013)	PRJNA594982(Acosta et al., 2020)
PRJNA234009(Cuthbertson et al., 2014)	PRJNA599290(Neerincx et al., 2021)
PRJNA271691(Carmody et al., 2015)	PRJNA604587(Valentini et al., 2020)
PRJNA288589(Hogan et al., 2016)	PRJNA611611(Lu et al., 2020)
PRJNA290694(Bacci et al., 2016)	PRJNA629006(Khalaf et al., 2021)
PRJNA360332(Whelan et al., 2017)	PRJNA645089
PRJNA387622(Peleg et al., 2018)	PRJNA662963(Heirali et al., 2020)
PRJNA423040(Carmody et al., 2018)	PRJNA666192(Zhao et al., 2020)
PRJNA433469(Soret et al., 2020)	PRJNA756039(Widder et al., 2022)

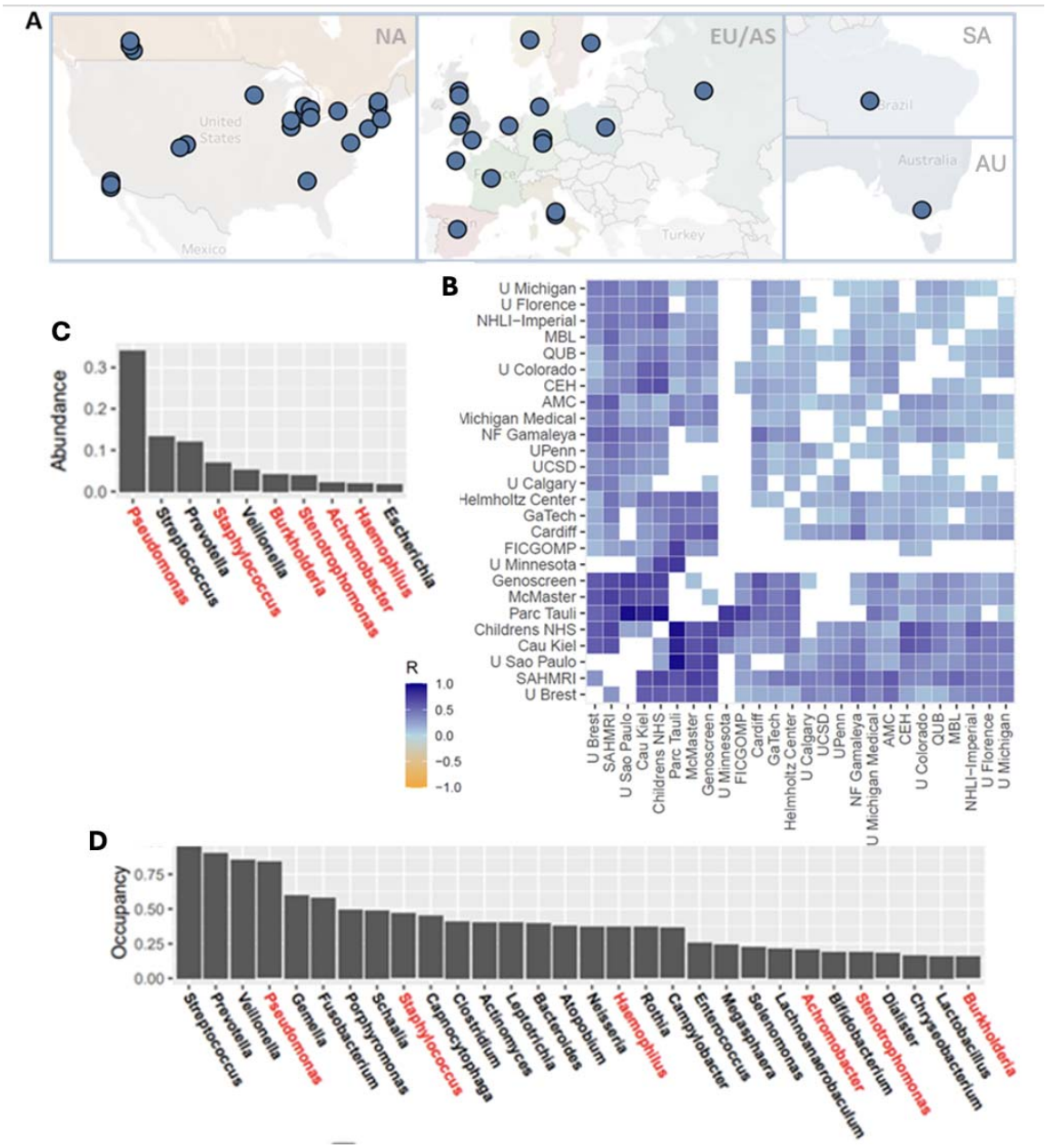

Figure 1 A multi-study CF database spanning 1184 pwCF and 4171 sputum samples. (**A**) We analyzed 36 studies across 26 CF centers from 14 countries worldwide. Three studies (PRJEB30646, PRJEB38277, and PRJNA207555) are split across more than one study site. (**B)** Pairwise ANOSIM R statistic for studies grouped by CF center that uploaded the study. White spaces denote pairs that were not significantly different ($p > 0.05$, Bonferroni corrected). (**C**) Mean relative abundance by genera. (**D**) Mean prevalence by genera. Canonical CF pathogens (*Pseudomonas, Staphylococcus, Burkholderia, Stenotrophomonas, Achromobacter,* and *Haemophilus*) are highlighted in red.

Post-rarefaction, 95% of reads came from 19 taxa. *Pseudomonas* was the most abundant taxa detected, followed by *Streptococcus*, *Prevotella*, and *Staphylococcus* (Figure 1C). *Streptococcus* was the most prevalent taxa, occurring in 95.3% of all samples, followed by *Prevotella*, *Veillonella*, and *Pseudomonas* (Figure 1D).

1184 CF microbiomes partition into 12 'pulmotypes' via DMM

To avoid over-representation by longitudinally tracked pwCF, we begin with a purely cross-sectional approach, taking only the first sample from each of the 1184 pwCF in our complete dataset. In brief, we filtered taxa by prevalence across studies (74 genera retained) and then used the specific DMM clustering algorithm used previously(Widder et al., 2022) to generate an 8 pulmotype schema (see methods for detailed processing and analysis steps).

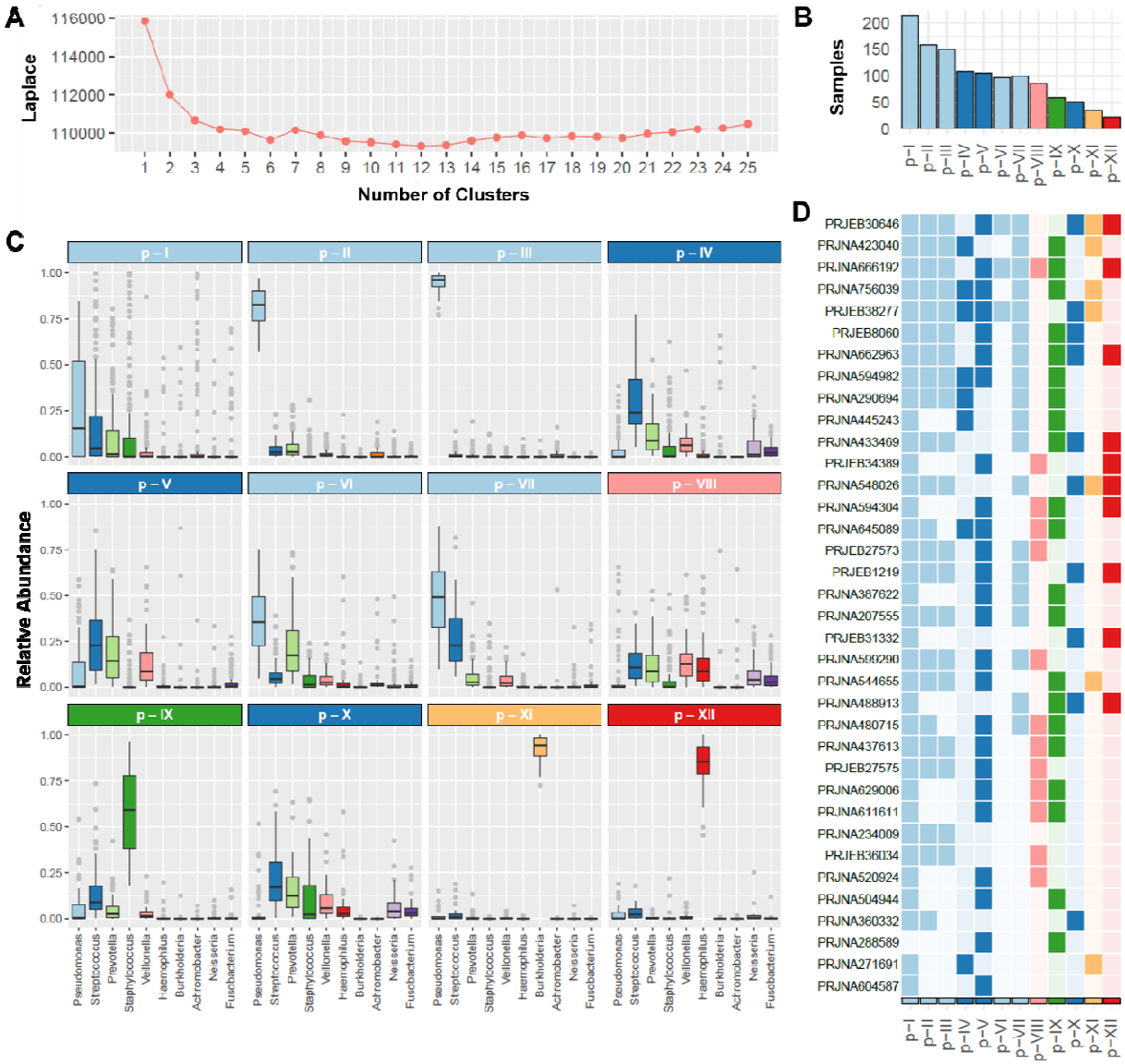

Figure 2. 1184 cystic fibrosis sputum microbiomes separate into 12 pulmotypes, via DMM. Clusters (k=1…25) were calculated using DMMs on individual snapshot data (N=1184) of the 74 most prevalent taxa, rarefied to 2000 sequences each. (**A**) Using the Laplace approximation of the negative log model evidence, we find a minimum at k=12 clusters (pulmotypes). (**B**) Overall frequency of each pulmotype across the initial 1184 samples. (**C**) Boxplots of the top 10 taxa grouped by 12 pulmotypes. (**D**) Pulmotypes represented in each study are shaded in. Studies are ordered by number of samples included.

Comparing the performance of one to 25 clusters, we find that CF lung microbiomes are best partitioned by DMM into twelve pulmotypes (Figure 2A-C), in contrast to prior studies

identifying 5(Hampton et al., 2021) or 8(Widder et al., 2022) pulmotypes. The optimal 12 pulmotype partitioning is detailed in Figure 2C (ordered by abundance), showing the relative abundances of the top-10 genera for each pulmotype. The count distribution across the 12 pulmotypes is shown in Figure 2B, with counts ranging from 16 to 214 samples per pulmotype.

We further organize our 12 clusters into 3 broad groups: **Pseudomonas-dominant (PA), oral commensal dominant (OC),** and **other pathogen dominant (OP).** The majority (60.7%) of the 1,184 samples are categorized as one of five PA-dominant pulmotypes (p-I, p-II, p-III, p-VI, and p-VII). The most common pulmotype is p-I (n = 214), which has moderate *Pseudomonas* relative abundance. Pulmotype p-III is the most homogeneous (DMM θ = 40.38; higher θ is more homogeneous) and typically exhibits over 90% *Pseudomonas*. By contrast, p-I is the least homogeneous (θ = 2.01) and contains a wide range of *Pseudomonas* levels. The PA pulmotypes also vary in overall *Pseudomonas* relative abundance (from lowest to highest: p-I, p-VI, p-VII, p-II, p-III). This pattern is consistent with a continuous gradation of *Pseudomonas* across samples arbitrarily clustered into distinct pulmotypes.

The four OC pulmotypes (p-IV, p-V, p-VIII, p-X) comprise 350 (29.5%) samples and are dominated by *Streptococcus* or *Veillonella*. Pathogen levels in the OC pulmotypes are generally low. Meanwhile, the three OP pulmotypes (p-IX, p-XI, and p-XII) total 115 samples (9.7%) and are dominated by non□*Pseudomonas* pathogens— namely *Staphylococcus* (p□IX), *Burkholderia* (p□XI), and *Haemophilus* (p□XII). Notably, we do not find a single OP pulmotype comprising *Stenotrophomonas*□dominated cases, despite loads exceeding 90% in

some samples. Instead, *Stenotrophomonas*□heavy samples are absorbed into p□I or p□III (both PA), or one of the OP clusters, rather than forming a separate pulmotype.

A risk of our multi-study approach is that clustering will simply separate pwCF by study. To begin to examine the validity and distinctness of the 12 pulmotypes, we first analyze their representation across included studies. In contrast to a major study effect on classification, we find that every pulmotype is represented in at least six studies, although no study contained all twelve pulmotypes (Figure 2D). The top four studies by number of pulmotypes represented (in decreasing order by total number: PRJNA423040, PRJNA756039, PRJEB30646, and PRJNA666192) were larger cross-sectional studies (pwCF > 57), including two that were used in prior pulmotyping analyses(Widder et al., 2022, Hampton et al., 2021).

Pulmotype classification is sensitive to database size and algorithm choice.

To summarize our initial analyses, the DMM method applied to 1184 pwCF produces 12 clusters that are broadly represented across individual studies (Figure 2). While the DMM pipeline supports a 12 cluster solution, we can see from Figure 2A that other clustering solutions (e.g. 11 and 13) are almost equally well supported. To assess the robustness of the 12 cluster solution, we next experiment by applying the same DMM method to repeated sub-samples of our dataset to establish confidence intervals on cluster number, and also to assess any dependency of cluster number on database size.

Figure 3 illustrates that when we repeat the same DMM clustering analysis on sub-samples of our 1184 pwCF dataset, we see consistency across replicates in cluster number for a given sample size, but also systematic variation as sample size changes (Figure 3). This strong

dependency on sample size provides a simple rationale for why our clustering scheme (Figure 2) has more clusters than an earlier study applying the same algorithm to a smaller dataset(Widder et al., 2022), or indeed different algorithms to smaller datasets (Hampton et al., 2021).

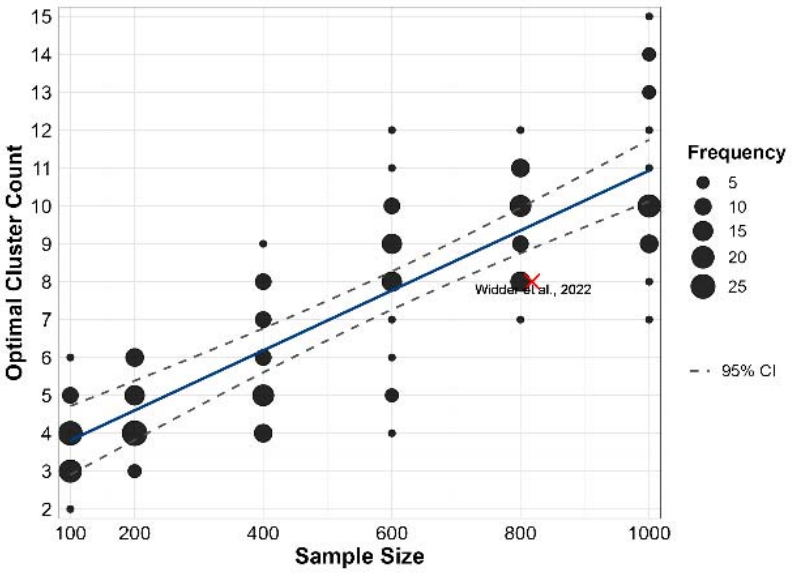

Figure 3. DMM clustering results are dependent on database size. The 1184 cross-sectional database was sub-sampled (without replacement) 60 times, for sample sizes ranging from 100 to 1000 pwCF. Points illustrate the optimal cluster count (analogous to the 12-cluster count in Figure 2), with point size illustrating the number of samples with the same cluster count (see inset). The blue line is a linear regression of mean cluster count on sample size, surrounded by 95% confidence interval (dotted lines). The red cross represents the DMM analysis by Widder et al. (Widder et al., 2022)(DMM clustering applied to 818 longitudinal samples from 109 pwCF).

To assess the potential role of algorithm choice, we next use our 1184 pwCF dataset to contrast DMM with other commonly-used clustering algorithms (k-means, and partitioning around medoids (PAM)). In Figure 4, we show that algorithm choice has a substantial effect on clustering outcome. For the same 1184 pwCF dataset, the resulting number of clusters varies from 2 (PAM) to 12 (DMM). Given the variability in clustering outcomes from a single dataset, an objective evaluation of algorithm performance is essential. We assess within-cluster cohesion

and between-cluster separation using the Average Silhouette Width (ASW) metric (Figure 4). Higher ASW scores for PAM indicate a more robust clustering scheme.

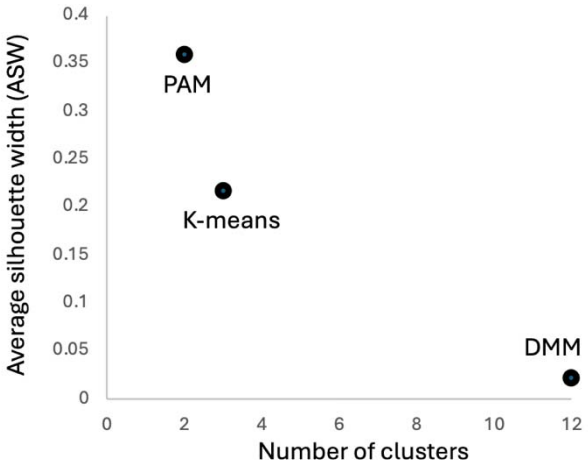

Figure 4. **cluster number and quality is dependent on algorithm choice.** The complete 1184 cross-sectional dataset was used to fit DMM, k-means and PAM (partitioning around medoids) clustering models. The x-axis indicates the number of clusters identified, while the y-axis indicates the Average Silhouette Width (ASW) score, a metric evaluating cluster quality, with a range from -1 to 1; higher scores denote stronger clustering (greater within-cluster homogeneity and between-cluster separation).

Our analysis in Figure 4 demonstrates that the PAM two-cluster scheme achieves higher clustering quality, as indicated by higher ASW scores. Building on this, we next evaluate the sensitivity of PAM clustering to database size, given our earlier finding that DMM clustering is size-dependent (Figure 3). As shown in Figure 5, unlike DMM clustering, PAM clustering remains highly robust across database sizes, consistently identifying the same two-cluster structure from 200 to 1000 pwCF. Notably, the composition of these clusters remains highly

conserved, further supporting the robustness of this classification.

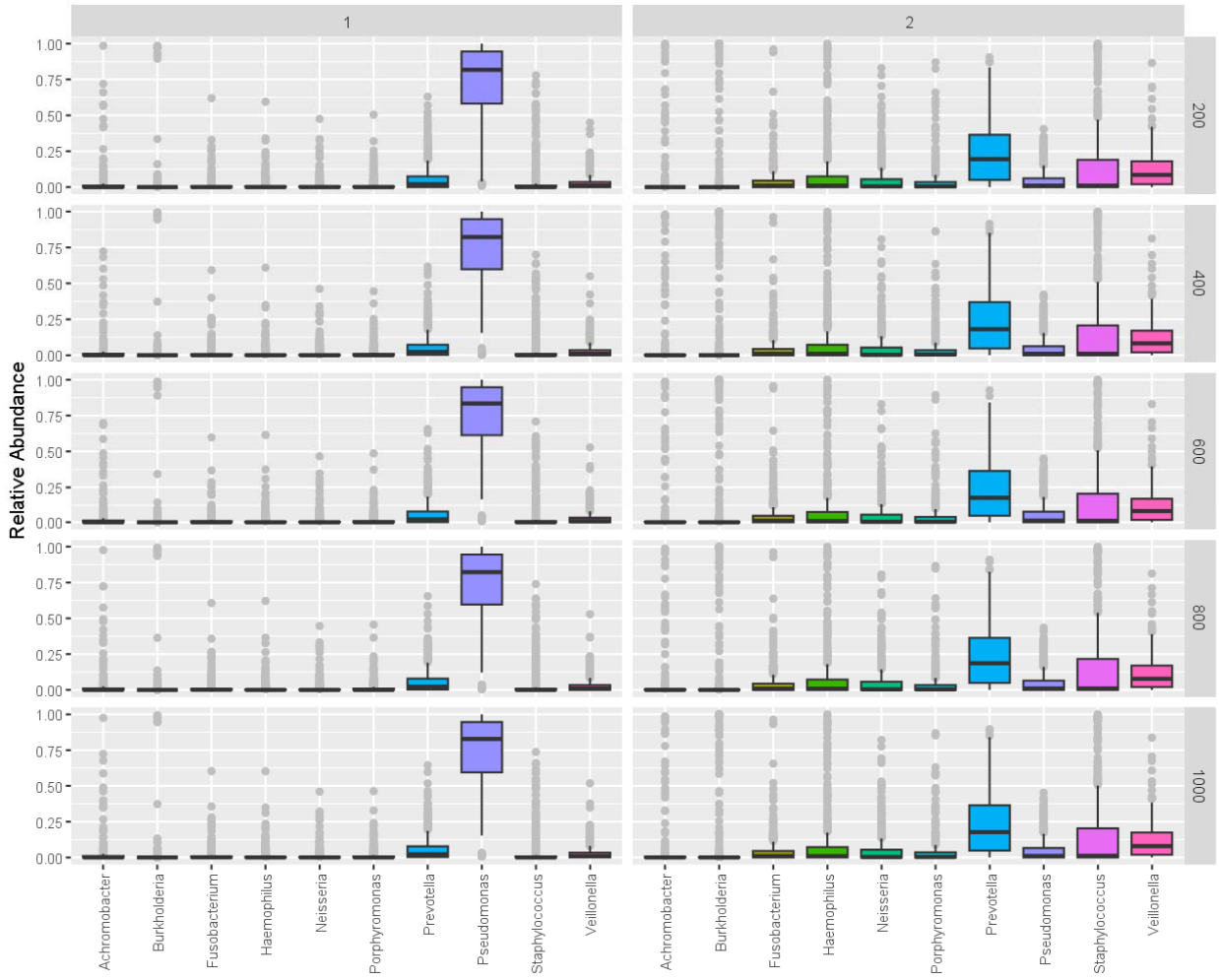

Figure 5. PAM clustering produces a repeatable 2 cluster schema, across database sizes. PAM clustering was repeated on single subsamples of our data, producing analyses on datasets ranging from 200 (top) to 1000 pwCF. For each PAM analysis, the optimal clustering partitioned the data into two clusters, with compositions detailed in the left panel (cluster 1) and the right panel (cluster 2). Each panel shows the relative abundance for the top 10 most abundant genera. The boxplots depict the variation in abundance of each genus within the identified clusters, with outliers indicated by grey dots.

Our analyses in Figures 4-5 indicate that a two-cluster model identified by PAM provides a robust classification scheme based on available cross-sectional data. Compositionally, this two-cluster model separates PA-dominant microbiomes (cluster 1, Figure 5) from all others (cluster

2). This distinction is consistent with the clinical weight placed on PA infections(Emerson et al., 2002) and is partially consistent with prior models differentiating ‘attack’ and ‘climax’ microbiome structures in pwCF, where PA has been associated with the climax community(Quinn et al., 2016, Conrad et al., 2013).

Clusters versus continua

Clustering algorithms always generate clustering solutions, regardless of whether the underlying data naturally forms discrete groups. Our ASW metric provides some insights into this issue, offering relative support for PAM clustering. Yet even in this most favorable case, the measured ASW is still relatively weak (below a suggested threshold of 0.5(Knights et al., 2014)), suggesting model misspecification. Since our PAM two-cluster model separates by PA abundance (Figure 5), we next assess the extent to which PA abundance forms a continuous (graded) or discrete (step-like) landscape across all 1184 initial timepoint samples (Figure 6). While we again see that clusters 1 and 2 are largely separable by PA relative abundance (Figures 5, 6), figure 6 shows that there is no sharp threshold in the abundance of PA across all samples, suggesting a continuous underlying landscape of variation.

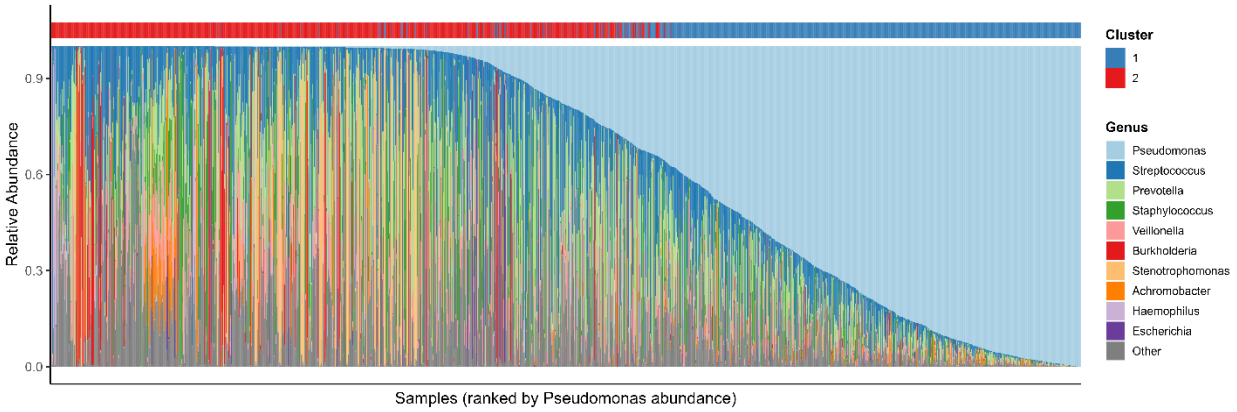

Figure 6. The PAM two cluster classification does not reflect a sharp boundary in *P. aeruginosa* abundance. Microbial community composition across samples ranked by *Pseudomonas* (PA) abundance. Each vertical bar represents a single sample, and the stacked colors within each bar correspond to the relative abundances of the top 10 most abundant bacterial genera, with all other genera combined into the "Other" category. Samples are ordered from left to right by increasing PA abundance (pale blue). A colored strip above the composition bars indicates the cluster assignment derived from partitioning around medoids (PAM) clustering.

Transition patterns in longitudinal data reveal a continuous landscape connecting DMM clusters.

Figures 2-6 show our analyses of initial timepoint data for 1184pwCF, revealing limitations for all clustering models. Broadly, our analysis points to a choice between a high-resolution twelve-cluster DMM model (but with low ASW scores and high sensitivity to dataset size, Figures 2-4), or a simple two-cluster PAM model (but with only marginal ASW improvement, Figures 4,5). In figure 6 we critique the underlying 'discrete space' pulmotyping assumption, by illustrating a clear compositional continuity across the major two-cluster border in the PAM model.

We now move on to our longitudinal sample dataset, to further evaluate a continuous space interpretation, where clusters partition an underlying continuous landscape of microbiome

variation. Under this interpretation, we hypothesize that longitudinal transitions in pulmotype cluster reflect underlying distances across a continuous microbiome landscape. To test this hypothesis, we focus on our twelve-pulmotype DMM partitioning (Figure 2), analyzing transitions within and between clusters, and cluster network properties. We use the 12-pulmotype DMM partition (Figure 2) as it provides a larger number of between-cluster transitions, also varying in cluster distances.

Using the prior 12-component DMM, which was fit to cross-sectional data alone, we classify the remaining 2,842 longitudinal samples (across 427 pwCF). Note that while we can infer ordinality (i.e. "which sample came first, second, etc…") across all subjects with longitudinal samples, we do not always have temporal information (i.e. "how many days passed between samples"). Among all pairs of consecutive samples (2,842 total), 1,686 (59.3%) show no change in pulmotype. Across all individual pwCF in our longitudinal dataset, we find that 125 pwCF (29.3%) do not transition to a new pulmotype during their surveillance period, and 197 pwCF (46.1%) do not change their pulmotype group (i.e. remaining with the broad classification of PA, OC, or OP dominated pulmotypes). Taken together, this indicates stability across pulmotype classification.

We next analyze the characteristics of pulmotype transitions between consecutive samples (Figure 7). For each of the 144 possible ordered pairs of pulmotypes we report the number of individuals in which we find that given transition across two consecutive samples (Figure 7A). We hypothesized that transitions in pulmotype state would result from either misclassification (samples drifting along pulmotype boundaries) or progressive (directional) community shifts. If misclassification is a substantial issue, we would expect to see a negative association between assignment confidence (the likelihood of observing a given sample in its

assigned DMM cluster) and the likelihood of a shift in pulmotype in the subsequent sample. In contrast, we find that within-pulmotype and between-pulmotype transitions do not differ in sample-pulmotype assignment confidence ($p=0.12$, Wilcoxon $W=20545$, Figure 7B), suggesting that pulmotype transitions are not substantially due to misclassification.

We next assess whether our classification supports a proximity model, where transitions are more common among pulmotypes that are more structurally similar (and thus have a smaller between-pulmotype distance). Consistent with this model we find that pairs of pulmotypes with lower Bray-Curtis dissimilarity experience more frequent transitions ($R=-0.34$, Figure 7C).

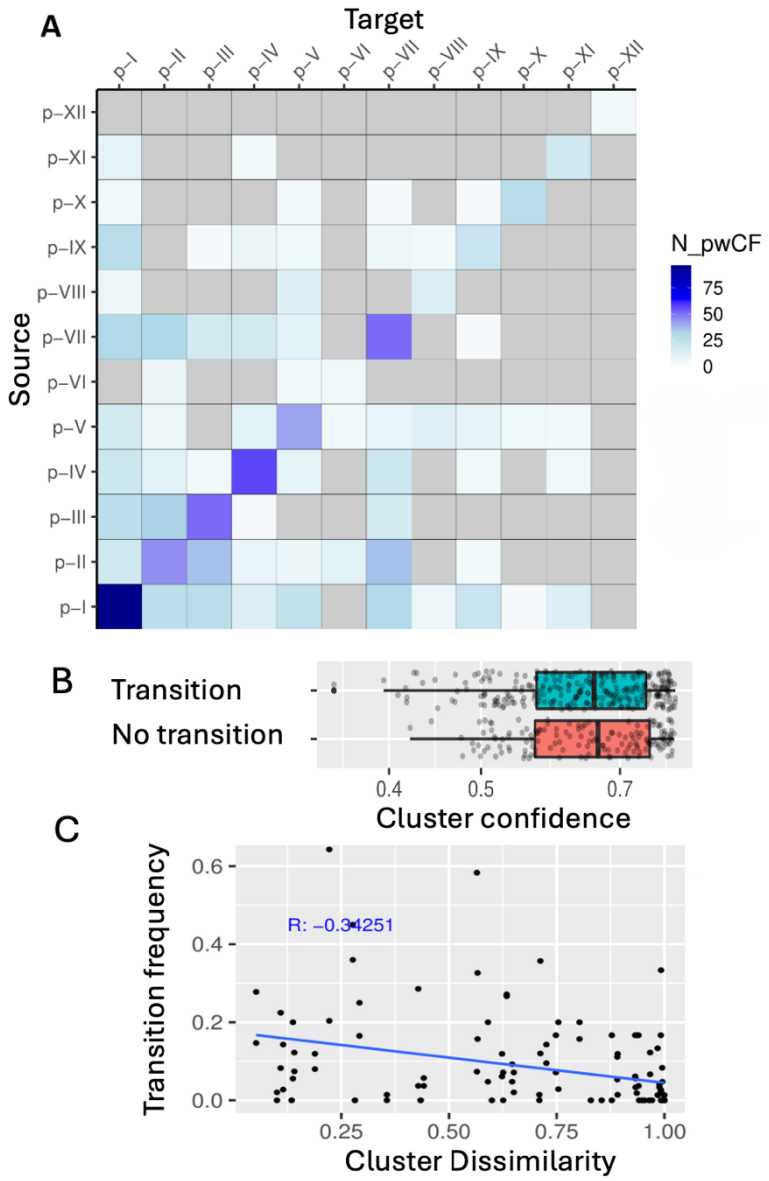

Figure 7. DMM pulmotype assignments are persistent in time, with greater transitions among more similar pulmotypes. We assess transition frequencies between pairs of consecutive samples for each pwCF. (**A**) Matrix of all transitions between pulmotypes, colored by the number of individuals a given transition was observed in. Following Widder et al.(Widder et al., 2022), all transitions with fewer than 3 observations were removed. (**B**) The pulmotype assignment confidence (the likelihood of observing a given sample in its assigned DMM cluster) is not different in between-pulmotype transitions compared to within-pulmotype transitions. (**C**) The transition frequency between two pulmotypes decreases with mean dissimilarity (ANOSIM R).

In light of Figure 7, we conclude that transitions among DMM clusters are in part a function of cluster distance, so that 'nearby' clusters (lower Bray Curtis dissimilarity) are more

likely to experience transitions (Figure 7D). We build on this interpretation by using cluster transition data (Figure 7A) to build a cluster transition network, where cluster-pairs with more frequent transitions are linked by a network edge (Figure 8). We threshold our network edges based on pulmotype assignment confidence, only including transitions where the product of source and target confidences exceeded 80%. This removes 819 transitions (28.8% of total transitions). Edges in the network are scaled by the number of pwCF for which a given transition was observed. Node sizes are scaled by frequency across the initial DMM training set (Figure 2B).

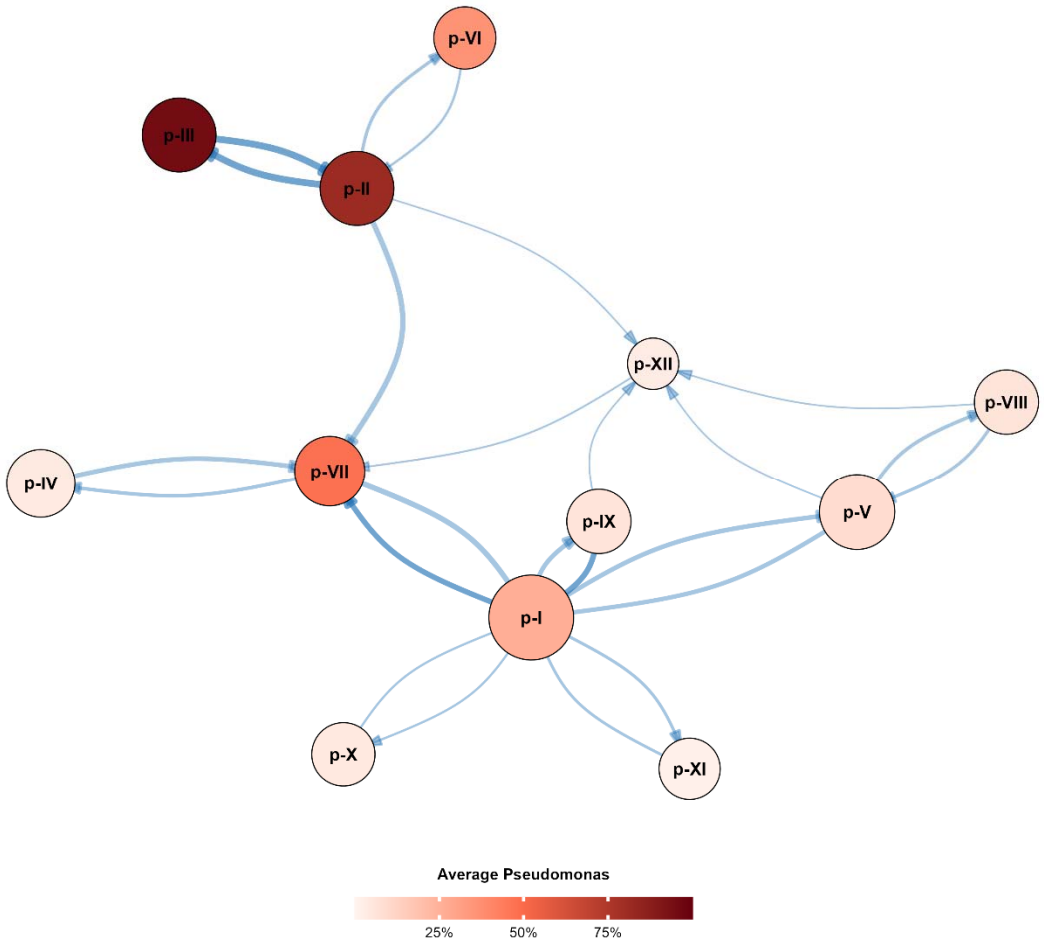

Figure 8. DMM pulmotype transitions form a structured bi-directional network, reflecting gradients in *P. aeruginosa* relative abundance. The network diagram shows each of the 12 DMM clusters as a node, with edges indicating observed transitions between clusters (thresholded by product of source and target assignment confidence > 80%). The node size reflects how many total samples were assigned to that cluster (larger nodes = more samples), and the node color is a gradient representing the average abundance of *Pseudomonas aeruginosa* in that cluster (darker indicates higher *Pseudomonas* levels, see heatmap inset). The edges are drawn with widths proportional to the transition frequency between clusters, and arrowheads denote the direction of the transition.

Our network visualization in Figure 8 reveals a backbone of ordered transitions in PA-dominant pulmotypes along a gradient of *P. aeruginosa* relative abundance, consistent with our earlier illustration of a continuous landscape of *P. aeruginosa* abundance (Figure 6). Figure 8

highlights that movement along this continuous gradient tends to be gradual, so that transition events tend to favor small step changes in *P. aeruginosa* abundance. Across all transitions in Figures 7 and 8, we find substantial bi-directionality (forward and reverse transition rates), indicating a general absence of progressive, directional change in pulmotypes through time. Figures 7 and 8 show frequent transitions from pathogen dominated (OP or PA) to oral commensal (OC) clusters, suggesting that pathogen dominanted clusters are not always ecological sinks (i.e., pwCF can and do escape from these states).

Discussion

In this study, we combined publicly available sputum sample microbiome data to identify consistent ecological patterns across over 1000 pwCF. We produce four key findings: (1) cluster partitioning is sensitive to both choice of algorithm and database size (Figures 2-6); (2) longitudinal time-series display clustering stasis (Figure 7); (3) Longitudinal transitions are biased towards similar clusters, e.g. movement along close gradations in *P. aeruginosa* dominance (Figure 7,8); (4) longitudinal cluster transitions show balanced bi-directionality, in contrast to the notion of progressive movement towards 'end state' pathogen dominance (Figures 7,8). The database assembled by this study is publicly available via GitHub (link) and represents a significant resource to both the CF community and for scientists engaged in the study of human associated microbiomes in the context of disease.

The field of CF has generated a substantial number of microbiome studies. These studies have identified complex microbial communities inhabiting CF airways with high between-person

and even within-person variability. In light of the multitude of generally low sample size studies (understandable given the limitations of clinical studies of rare genetic conditions), composite studies are potentially beneficial in identifying broad-scale patterns across numerous cohorts. For example, Li et al. performed a data mining analysis across 18 studies with 718 sputum samples and found that overall, antibiotic treatments for exacerbation management had a large impact on commensal taxa but little impact on CF pathogens(Li et al., 2016).

As reviewed earlier, we are not the first study to apply pulmotyping to CF(Widder et al., 2022, Hampton et al., 2021). Together these variable prior classifications underline our conclusion that clustering solutions are highly sensitive to choice of clustering algorithm and constraints on the amount of available data (Figures 2-5). In the specific case of DMM clustering, our results in Figure 2 compared to Widder et al. (Widder et al., 2022) suggest that more data buys greater resolution of what is fundamentally a continuous landscape of underlying variation (Figure 3).

To conduct a longitudinal analysis we used our 12-cluster DMM partitioning (Figure 2), as it offered a higher cluster number and therefore the potential for more transitions and a more complex transition network (Figures 7,8). Our result that cluster transitions are substantially bi-directional (Figures 7,8) is consistent with (Widder et al., 2022), and raises the question of what processes drive exits from potentially ‘end stage’ pathogen dominated states (notably DMM clusters II, III (heavy *P. aeruginosa* dominance) and XI (*Burkholderia* dominance). We speculate that the transitions between PA states with higher *Pseudomonas* loads to lower ones corresponds to antibiotic treatment, as similar transitions were identified in (Widder et al., 2022). This is consistent with the notion that antibiotic treatment of *Pseudomonas* leads to variable

outcomes(Somayaji et al., 2019), potentially either reducing pathogen loads to a more oral commensal-dominant state, or potentially allow for competitive release of other pathogens(Varga et al., 2022, Waldetoft et al., 2022) and therefore promote transitions into distinct pulmotypes. We were ultimately unable to assess this hypothesis given a lack of published, standardized antibiotic information, and we suggest that the field move towards recording and sharing antibiotic prescription data where possible to aid in future studies.

In this paper we have developed and applied a robust pipeline to generate a combined dataset of unprecedented size in CF research, representing over 1000 pwCF and over 4000 samples. Using the dataset, we show that microbiome clustering solutions are dependent on both choice of algorithm and scale of data (Figures 2-6). While specific clustering solutions are variable, we provide evidence that the underlying continuous variation in microbiome structure forms an ordered landscape, characterized by preferential bi-directional transitions to nearby states (Figures 7,8).

Acknowledgements.

We thank Arlene Stecenko, Joshua Weitz, Peng Qiu and members of the Brown lab for helpful feedback on previous drafts. We thank the Cystic Fibrosis Foundation (awards BROWN23I0, BROWN21P0) and the CDC (75D30120C09782) for funding this work.

Methods

Dataset Curation

On February 9th, 2022 we searched NCBI-SRA for 16S-sequenced sputum surveys of CF lung microbiomes using the following query:

```
(((cystic fibrosis OR cf) AND (lung OR respiratory OR sputum OR
airway))) AND (amplicon[Strategy] OR other[Strategy]).
```

This returned 107 potential BioProject numbers. We manually searched for corresponding publications for each repository and excluded all studies that lacked corresponding methods or any information to match sputum samples with sample donor information. BioProjects that were not demultiplexed before SRA submission were excluded from this study.

In total, 36 BioProjects passed our inclusion criteria. For each BioProject, we used the same pipeline. All function parameters were set to defaults unless otherwise noted. First, we pulled all associated sample fastq files. As studies sequenced different 16S regions using different primers, we standardize all sequences by applying a uniform quality filter (maxEE=5) and trimming the first 20bp and truncating to 140bp (trimLeft=20; truncLen=140) using the dada2::filterAndTrim function in R, with the remaining parameters set to defaults. Samples for which fewer than 20% of the reads passed this sequencing quality filter were discarded.

To optimize the dada2 error inference step, we included all samples that passed our filters, including non-sputum samples. We used dada2::dada to infer sequencing error rates and removed chimeras using dada2::removeBimeraDenovo. We assigned taxonomy by BLASTing each sequence against the NCBI 16S ribosomal RNA database, identifying the top 10 alignments, and reporting the most frequent genus call. All subsequent data handling was built using the phyloseq packages in R. We successfully analyzed 5201 samples using this pipeline and subsequently removed non-sputum samples such as sequencing controls and paired samples from other body sites, as well as non-observational (experimentally manipulated) samples from further downstream analysis.

The resulting dataset contained 4171 sputum samples with manually curated and matched sample metadata. Sputum samples contained a median of 20061 reads (median 19497, range 1045-1264313). DNA sequences were assigned to 1090 distinct genera. To mitigate study-specific sequencing bias, we only analyze genera that were detected across the majority (>18) of studies. This yielded 74 genera across our dataset for downstream analysis. To account for the variability in total read output for each individual study, all samples were then subsampled to a sequencing depth of 2000 reads; 145 samples were below this read threshold and thus discarded, yielding 4026 sputum samples across 1184 subjects.

Dirichlet Multinomial Modeling

Following the procedure outlined in Holmes et al. (Holmes et al., 2012), we partition samples into pulmotypes using Dirichlet Multinomial Mixture (DMM) modeling. DMMs have been used to perform unsupervised clustering on microbiome datasets across numerous contexts(Costea et al., 2018, Holmes et al., 2012, Widder et al., 2022). We fit DMMs using the DirichletMultinomial R package. To avoid individual over-representation, we only include the earliest available sputum sample for each subject during model training. Cluster assignment confidence was calculated as the likelihood of observing a given sample in its maximally likely component in the fit DMM model.

Partitioning Around Medoids (PAM)

Following the procedure outlined in Kaufman and Rousseeuw(Kaufman and Rousseeuw, 2009), we partition samples into pulmotypes using Partitioning Around Medoids (PAM). PAM has been applied for unsupervised clustering in a variety of microbiome studies(Arumugam et al., 2011,

Sun et al., 2025, Acosta et al., 2018). We implement PAM through the ‘cluster’ R package, maximizing the Calinski–Harabasz (CH) index to determine the optimal number of clusters. To avoid individual over-representation, we only include the earliest available sputum sample for each subject during model training. Cluster assignment confidence is evaluated by calculating the mean silhouette width, reflecting each sample’s similarity to its assigned cluster relative to other clusters.

K-means model

Following the procedure introduced by MacQueen(MacQueen, 1967), we partition samples into pulmotypes using **K-means**. K-means has been employed commonly for unsupervised clustering across microbiome studies(Hampton et al., 2021, Boutin et al., 2017). We implement K-means through the base R ‘stats’ package, systematically testing different values of *k* (e.g., 2 to 20) and applying the **elbow method** to determine the optimal number of clusters (the “elbow” in the plot of within-cluster sum of squares versus *k*). To avoid individual over-representation, we only include the earliest available sputum sample from each subject during model training. Cluster assignment confidence is assessed by **mean silhouette width**, which measures how similar each sample is to its assigned cluster compared to other clusters.

Average Silhouette Width (ASW)

Following the procedure introduced by Rousseeuw(Rousseeuw, 1987), we measure cluster separation by computing the **Average Silhouette Width (ASW)**. ASW captures how similar each sample is to its own cluster relative to the nearest alternative cluster, and then averages this value across all samples. To avoid individual over-representation, we only include each subject’s

earliest sputum sample for model training. We additionally compare discovery-set silhouettes (swDiscov) to validation-set silhouettes (swValid), quantifying their difference (swDiff) as an indicator of cluster robustness: positive swDiff suggests stable generalization, whereas negative swDiff may signal overfitting.

Compositional differences

We test for compositionally distinct studies using a leave-one-out approach. Analysis of similiarty (ANOSIM) tests were performed on Bray-Curtis distances between each study and the composite of all other studies using the anosim function in the vegan R package(Oksanen et al., 2023). We then aggregate studies by reporting clinical center and perform both leave-one-out and pairwise center comparisons using ANOSIM. We also test pulmotype compositional differences using pairwise ANOSIM tests. For each set of comparisons, significance was assessed at $p=0.05$ (Bonferroni-corrected). Meaningful effect sizes were assessed at $R>0.4$ (Roberts et al., 2008).

REFERENCES

ACOSTA, N., HEIRALI, A., SOMAYAJI, R., SURETTE, M. G., WORKENTINE, M. L., SIBLEY, C. D., RABIN, H. R. & PARKINS, M. D. 2018. Sputum microbiota is predictive of long-term clinical outcomes in young adults with cystic fibrosis. *Thorax,* 73**,** 1016-1025.

ACOSTA, N., WADDELL, B., HEIRALI, A., SOMAYAJI, R., SURETTE, M. G., WORKENTINE, M. L., RABIN, H. R. & PARKINS, M. D. 2020. Cystic Fibrosis Patients Infected With Epidemic Pseudomonas aeruginosa Strains Have Unique Microbial Communities. *Front Cell Infect Microbiol,* 10**,** 173.

ARUMUGAM, M., RAES, J., PELLETIER, E., LE PASLIER, D., YAMADA, T., MENDE, D. R., FERNANDES, G. R., TAP, J., BRULS, T., BATTO, J. M., BERTALAN, M., BORRUEL, N., CASELLAS, F., FERNANDEZ, L., GAUTIER, L., HANSEN, T., HATTORI, M., HAYASHI, T., KLEEREBEZEM, M., KUROKAWA, K., LECLERC, M., LEVENEZ, F., MANICHANH, C., NIELSEN, H. B., NIELSEN, T., PONS, N., POULAIN, J., QIN, J., SICHERITZ-PONTEN, T., TIMS, S., TORRENTS, D., UGARTE, E., ZOETENDAL, E. G., WANG, J., GUARNER, F., PEDERSEN, O., DE VOS, W. M., BRUNAK, S., DORÉ, J., ANTOLÍN, M., ARTIGUENAVE, F., BLOTTIERE, H. M., ALMEIDA, M., BRECHOT, C., CARA, C., CHERVAUX, C., CULTRONE, A., DELORME, C., DENARIAZ, G., DERVYN, R., FOERSTNER, K. U., FRISS, C., VAN DE GUCHTE, M., GUEDON, E., HAIMET, F., HUBER, W., VAN HYLCKAMA-VLIEG, J., JAMET, A., JUSTE, C., KACI, G., KNOL, J., LAKHDARI, O., LAYEC, S., LE ROUX, K., MAGUIN, E., MÉRIEUX, A., MELO MINARDI, R., M'RINI, C., MULLER, J., OOZEER, R., PARKHILL, J., RENAULT, P., RESCIGNO, M., SANCHEZ, N., SUNAGAWA, S., TORREJON, A., TURNER, K., VANDEMEULEBROUCK, G., VARELA, E., WINOGRADSKY, Y., ZELLER, G., WEISSENBACH, J., EHRLICH, S. D. & BORK, P. 2011. Enterotypes of the human gut microbiome. *Nature,* 473**,** 174-80.

BACCI, G., PAGANIN, P., LOPEZ, L., VANNI, C., DALMASTRI, C., CANTALE, C., DADDIEGO, L., PERROTTA, G., DOLCE, D., MORELLI, P., TUCCIO, V., DE ALESSANDRI, A., FISCARELLI, E. V., TACCETTI, G., LUCIDI, V., BEVIVINO, A. & MENGONI, A. 2016. Pyrosequencing Unveils Cystic Fibrosis Lung Microbiome Differences Associated with a Severe Lung Function Decline. *PLoS One,* 11**,** e0156807.

BOUTIN, S., HAGENFELD, D., ZIMMERMANN, H., EL SAYED, N., HÖPKER, T., GREISER, H. K., BECHER, H., KIM, T. S. & DALPKE, A. H. 2017. Clustering of Subgingival Microbiota Reveals Microbial Disease Ecotypes Associated with Clinical Stages of Periodontitis in a Cross-Sectional Study. *Front Microbiol,* 8**,** 340.

CARMODY, L. A., CAVERLY, L. J., FOSTER, B. K., ROGERS, M. A. M., KALIKIN, L. M., SIMON, R. H., VANDEVANTER, D. R. & LIPUMA, J. J. 2018. Fluctuations in airway bacterial communities associated with clinical states and disease stages in cystic fibrosis. *PLoS One,* 13**,** e0194060.

CARMODY, L. A., ZHAO, J., KALIKIN, L. M., LEBAR, W., SIMON, R. H., VENKATARAMAN, A., SCHMIDT, T. M., ABDO, Z., SCHLOSS, P. D. & LIPUMA,

J. J. 2015. The daily dynamics of cystic fibrosis airway microbiota during clinical stability and at exacerbation. *Microbiome,* 3**,** 12.

CAVERLY, L. J., LU, J., CARMODY, L. A., KALIKIN, L. M., SHEDDEN, K., OPRON, K., AZAR, M., CAHALAN, S., FOSTER, B., VANDEVANTER, D. R., SIMON, R. H. & LIPUMA, J. J. 2019. Measures of Cystic Fibrosis Airway Microbiota during Periods of Clinical Stability. *Ann Am Thorac Soc,* 16**,** 1534-1542.

CAVERLY, L. J., ZHAO, J. & LIPUMA, J. J. 2015. Cystic fibrosis lung microbiome: Opportunities to reconsider management of airway infection. *Pediatric Pulmonology,* 50**,** S31-S38.

CAVERLY, L. J., ZIMBRIC, M., AZAR, M., OPRON, K. & LIPUMA, J. J. 2021. Cystic fibrosis airway microbiota associated with outcomes of nontuberculous mycobacterial infection. *ERJ Open Res,* 7.

COBURN, B., WANG, P. W., DIAZ CABALLERO, J., CLARK, S. T., BRAHMA, V., DONALDSON, S., ZHANG, Y., SURENDRA, A., GONG, Y., ELIZABETH TULLIS, D., YAU, Y. C., WATERS, V. J., HWANG, D. M. & GUTTMAN, D. S. 2015. Lung microbiota across age and disease stage in cystic fibrosis. *Sci Rep,* 5**,** 10241.

CONRAD, D., HAYNES, M., SALAMON, P., RAINEY, P. B., YOULE, M. & ROHWER, F. 2013. Cystic fibrosis therapy: a community ecology perspective. *Am J Respir Cell Mol Biol,* 48**,** 150-6.

COSTEA, P. I., HILDEBRAND, F., ARUMUGAM, M., BÄCKHED, F., BLASER, M. J., BUSHMAN, F. D., DE VOS, W. M., EHRLICH, S. D., FRASER, C. M., HATTORI, M., HUTTENHOWER, C., JEFFERY, I. B., KNIGHTS, D., LEWIS, J. D., LEY, R. E., OCHMAN, H., O'TOOLE, P. W., QUINCE, C., RELMAN, D. A., SHANAHAN, F., SUNAGAWA, S., WANG, J., WEINSTOCK, G. M., WU, G. D., ZELLER, G., ZHAO, L., RAES, J., KNIGHT, R. & BORK, P. 2018. Enterotypes in the landscape of gut microbial community composition. *Nature Microbiology,* 3**,** 8-16.

CUTHBERTSON, L., ROGERS, G. B., WALKER, A. W., OLIVER, A., GREEN, L. E., DANIELS, T. W., CARROLL, M. P., PARKHILL, J., BRUCE, K. D. & VAN DER GAST, C. J. 2016. Respiratory microbiota resistance and resilience to pulmonary exacerbation and subsequent antimicrobial intervention. *Isme j,* 10**,** 1081-91.

CUTHBERTSON, L., ROGERS, G. B., WALKER, A. W., OLIVER, A., HAFIZ, T., HOFFMAN, L. R., CARROLL, M. P., PARKHILL, J., BRUCE, K. D. & VAN DER GAST, C. J. 2014. Time between collection and storage significantly influences bacterial sequence composition in sputum samples from cystic fibrosis respiratory infections. *J Clin Microbiol,* 52**,** 3011-6.

CUTHBERTSON, L., WALKER, A. W., OLIVER, A. E., ROGERS, G. B., RIVETT, D. W., HAMPTON, T. H., ASHARE, A., ELBORN, J. S., DE SOYZA, A., CARROLL, M. P., HOFFMAN, L. R., LANYON, C., MOSKOWITZ, S. M., O'TOOLE, G. A., PARKHILL, J., PLANET, P. J., TENEBACK, C. C., TUNNEY, M. M., ZUCKERMAN, J. B., BRUCE, K. D. & VAN DER GAST, C. J. 2020. Lung function and microbiota diversity in cystic fibrosis. *Microbiome,* 8**,** 45.

EMERSON, J., ROSENFELD, M., MCNAMARA, S., RAMSEY, B. & GIBSON, R. L. 2002. Pseudomonas aeruginosa and other predictors of mortality and morbidity in young children with cystic fibrosis. *Pediatric pulmonology,* 34**,** 91-100.

FLYNN, J. M., NICCUM, D., DUNITZ, J. M. & HUNTER, R. C. 2016. Evidence and Role for Bacterial Mucin Degradation in Cystic Fibrosis Airway Disease. *PLoS Pathog,* 12**,** e1005846.

GARCIA-NUÑEZ, M., GARCIA-GONZALEZ, M., POMARES, X., MONTÓN, C., MILLARES, L., QUERO, S., PRINA, E., ASENSIO, O., BOSQUE, M., CAPILLA, S., CUEVAS, O. & MONSÓ, E. 2020. The Respiratory Microbiome in Cystic Fibrosis: Compartment Patterns and Clinical Relationships in Early Stage Disease. *Front Microbiol,* 11**,** 1463.

GODDARD, A. F., STAUDINGER, B. J., DOWD, S. E., JOSHI-DATAR, A., WOLCOTT, R. D., AITKEN, M. L., FLIGNER, C. L. & SINGH, P. K. 2012. Direct sampling of cystic fibrosis lungs indicates that DNA-based analyses of upper-airway specimens can misrepresent lung microbiota. *Proc Natl Acad Sci U S A,* 109**,** 13769-74.

GRAHL, N., DOLBEN, E. L., FILKINS, L. M., CROCKER, A. W., WILLGER, S. D., MORRISON, H. G., SOGIN, M. L., ASHARE, A., GIFFORD, A. H., JACOBS, N. J., SCHWARTZMAN, J. D. & HOGAN, D. A. 2018. Profiling of Bacterial and Fungal Microbial Communities in Cystic Fibrosis Sputum Using RNA. *mSphere,* 3.

HAHN, A., FANOUS, H., JENSEN, C., CHANEY, H., SAMI, I., PEREZ, G. F., KOUMBOURLIS, A. C., LOUIE, S., BOST, J. E., VAN DEN ANKER, J. N., FREISHTAT, R. J., ZEMANICK, E. T. & CRANDALL, K. A. 2019. Changes in microbiome diversity following beta-lactam antibiotic treatment are associated with therapeutic versus subtherapeutic antibiotic exposure in cystic fibrosis. *Scientific Reports,* 9**,** 2534.

HAMPTON, T. H., THOMAS, D., VAN DER GAST, C., O'TOOLE, G. A. & STANTON, B. A. 2021. Mild Cystic Fibrosis Lung Disease Is Associated with Bacterial Community Stability. *Microbiology Spectrum,* 9**,** 10.1128/spectrum.00029-21.

HEIRALI, A., THORNTON, C., ACOSTA, N., SOMAYAJI, R., LAFOREST LAPOINTE, I., STOREY, D., RABIN, H., WADDELL, B., ROSSI, L., ARRIETA, M. C., SURETTE, M. & PARKINS, M. D. 2020. Sputum microbiota in adults with CF associates with response to inhaled tobramycin. *Thorax,* 75**,** 1058-1064.

HOGAN, D. A., WILLGER, S. D., DOLBEN, E. L., HAMPTON, T. H., STANTON, B. A., MORRISON, H. G., SOGIN, M. L., CZUM, J. & ASHARE, A. 2016. Analysis of Lung Microbiota in Bronchoalveolar Lavage, Protected Brush and Sputum Samples from Subjects with Mild-To-Moderate Cystic Fibrosis Lung Disease. *PLOS ONE,* 11**,** e0149998.

HOLMES, I., HARRIS, K. & QUINCE, C. 2012. Dirichlet Multinomial Mixtures: Generative Models for Microbial Metagenomics. *PLOS ONE,* 7**,** e30126.

JEAN-PIERRE, F., HAMPTON, T. H., SCHULTZ, D., HOGAN, D. A., GROLEAU, M.-C., DÉZIEL, E. & O'TOOLE, G. A. 2023. Community composition shapes microbial-specific phenotypes in a cystic fibrosis polymicrobial model system. *eLife,* 12**,** e81604.

JORTH, P., EHSAN, Z., REZAYAT, A., CALDWELL, E., POPE, C., BREWINGTON, J. J., GOSS, C. H., BENSCOTER, D., CLANCY, J. P. & SINGH, P. K. 2019. Direct Lung Sampling Indicates That Established Pathogens Dominate Early Infections in Children with Cystic Fibrosis. *Cell Rep,* 27**,** 1190-1204.e3.

KAUFMAN, L. & ROUSSEEUW, P. J. 2009. *Finding groups in data: an introduction to cluster analysis,* John Wiley & Sons.

KERAVEC, M., MOUNIER, J., GUILLOUX, C. A., FANGOUS, M. S., MONDOT, S., VALLET, S., GOURIOU, S., LE BERRE, R., RAULT, G., FÉREC, C., BARBIER, G., LEPAGE, P. & HÉRY-ARNAUD, G. 2019. Porphyromonas, a potential predictive biomarker of Pseudomonas aeruginosa pulmonary infection in cystic fibrosis. *BMJ Open Respir Res,* 6**,** e000374.

KHALAF, R. T., FURUTA, G. T., WAGNER, B. D., ROBERTSON, C. E., ANDREWS, R., STEVENS, M. J., FILLON, S. A., ZEMANICK, E. T. & HARRIS, J. K. 2021. Influence of Acid Blockade on the Aerodigestive Tract Microbiome in Children With Cystic Fibrosis. *J Pediatr Gastroenterol Nutr,* 72**,** 520-527.

KNIGHTS, D., WARD, T. L., MCKINLAY, C. E., MILLER, H., GONZALEZ, A., MCDONALD, D. & KNIGHT, R. 2014. Rethinking "enterotypes". *Cell Host Microbe,* 16**,** 433-7.

KRAMER, R., SAUER-HEILBORN, A., WELTE, T., JAUREGUI, R., BRETTAR, I., GUZMAN, C. A. & HÖFLE, M. G. 2015. High Individuality of Respiratory Bacterial Communities in a Large Cohort of Adult Cystic Fibrosis Patients under Continuous Antibiotic Treatment. *PLOS ONE,* 10**,** e0117436.

LI, J., HAO, C., REN, L., XIAO, Y., WANG, J. & QIN, X. 2016. Data Mining of Lung Microbiota in Cystic Fibrosis Patients. *PLoS One,* 11**,** e0164510.

LU, J., CARMODY, L. A., OPRON, K., SIMON, R. H., KALIKIN, L. M., CAVERLY, L. J. & LIPUMA, J. J. 2020. Parallel Analysis of Cystic Fibrosis Sputum and Saliva Reveals Overlapping Communities and an Opportunity for Sample Decontamination. *mSystems,* 5.

MACQUEEN, J. Some methods for classification and analysis of multivariate observations. Proceedings of the Fifth Berkeley Symposium on Mathematical Statistics and Probability, Volume 1: Statistics, 1967. University of California press, 281-298.

MAESTRALI, F., PILAN, R., ATHANAZIO, R., SPARVOLI, L., CORTEZ, R., TADDEI, C. & VOEGELS, R. 2020. Cystic fibrosis microbiome: analysis of nasal middle meatus and sputum in different lung disease stages. *Rhinology Online,* 3**,** 225-237.

NEERINCX, A. H., WHITESON, K., PHAN, J. L., BRINKMAN, P., ABDEL-AZIZ, M. I., WEERSINK, E. J. M., ALTENBURG, J., MAJOOR, C. J., MAITLAND-VAN DER ZEE, A. H. & BOS, L. D. J. 2021. Lumacaftor/ivacaftor changes the lung microbiome and metabolome in cystic fibrosis patients. *ERJ Open Res,* 7.

OKSANEN, J., SIMPSON, G., BLANCHET, F., KINDT, R., LEGENDRE, P., MINCHIN, P., O'HARA, R., SOLYMOS, P., STEVENS, M. & SZOECS, E. 2023. vegan: Community Ecology Package. R package version 2.6-4. 2022. Github.

PELEG, A. Y., CHOO, J. M., LANGAN, K. M., EDGEWORTH, D., KEATING, D., WILSON, J., ROGERS, G. B. & KOTSIMBOS, T. 2018. Antibiotic exposure and interpersonal variance mask the effect of ivacaftor on respiratory microbiota composition. *J Cyst Fibros,* 17**,** 50-56.

PRICE, K. E., HAMPTON, T. H., GIFFORD, A. H., DOLBEN, E. L., HOGAN, D. A., MORRISON, H. G., SOGIN, M. L. & O'TOOLE, G. A. 2013. Unique microbial communities persist in individual cystic fibrosis patients throughout a clinical exacerbation. *Microbiome,* 1**,** 27.

QUINN, R. A., ADEM, S., MILLS, R. H., COMSTOCK, W., DERIGHT GOLDASICH, L., HUMPHREY, G., AKSENOV, A. A., MELNIK, A. V., DA SILVA, R., ACKERMANN, G., BANDEIRA, N., GONZALEZ, D. J., CONRAD, D., O'DONOGHUE, A. J.,

KNIGHT, R. & DORRESTEIN, P. C. 2019. Neutrophilic proteolysis in the cystic fibrosis lung correlates with a pathogenic microbiome. *Microbiome,* 7**,** 23.

QUINN, R. A., COMSTOCK, W., ZHANG, T., MORTON, J. T., DA SILVA, R., TRAN, A., AKSENOV, A., NOTHIAS, L.-F., WANGPRASEURT, D., MELNIK, A. V., ACKERMANN, G., CONRAD, D., KLAPPER, I., KNIGHT, R. & DORRESTEIN, P. C. 2018. Niche partitioning of a pathogenic microbiome driven by chemical gradients. *Science Advances,* 4**,** eaau1908.

QUINN, R. A., WHITESON, K., LIM, Y. W., ZHAO, J., CONRAD, D., LIPUMA, J. J., ROHWER, F. & WIDDER, S. 2016. Ecological networking of cystic fibrosis lung infections. *NPJ Biofilms Microbiomes,* 2**,** 4.

RAGHUVANSHI, R., VASCO, K., VÁZQUEZ-BAEZA, Y., JIANG, L., MORTON, J. T., LI, D., GONZALEZ, A., GOLDASICH, L. D., HUMPHREY, G., ACKERMANN, G., SWAFFORD, A. D., CONRAD, D., KNIGHT, R., DORRESTEIN, P. C. & QUINN, R. A. 2020. High-Resolution Longitudinal Dynamics of the Cystic Fibrosis Sputum Microbiome and Metabolome through Antibiotic Therapy. *mSystems,* 5**,** 10.1128/msystems.00292-20.

ROBERTS, J. M., HENRY, L.-A., LONG, D. & HARTLEY, J. P. 2008. Cold-water coral reef frameworks, megafaunal communities and evidence for coral carbonate mounds on the Hatton Bank, north east Atlantic. *Facies,* 54**,** 297-316.

RONCHETTI, K., TAME, J. D., PAISEY, C., THIA, L. P., DOULL, I., HOWE, R., MAHENTHIRALINGAM, E. & FORTON, J. T. 2018. The CF-Sputum Induction Trial (CF-SpIT) to assess lower airway bacterial sampling in young children with cystic fibrosis: a prospective internally controlled interventional trial. *Lancet Respir Med,* 6**,** 461-471.

ROUSSEEUW, P. J. 1987. Silhouettes: A graphical aid to the interpretation and validation of cluster analysis. *Journal of Computational and Applied Mathematics,* 20**,** 53-65.

SOMAYAJI, R., PARKINS, M. D., SHAH, A., MARTINIANO, S. L., TUNNEY, M. M., KAHLE, J. S., WATERS, V. J., ELBORN, J. S., BELL, S. C., FLUME, P. A. & VANDEVANTER, D. R. 2019. Antimicrobial susceptibility testing (AST) and associated clinical outcomes in individuals with cystic fibrosis: A systematic review. *J Cyst Fibros,* 18**,** 236-243.

SORET, P., VANDENBORGHT, L.-E., FRANCIS, F., CORON, N., ENAUD, R., AVALOS, M., SCHAEVERBEKE, T., BERGER, P., FAYON, M., THIEBAUT, R., DELHAES, L., CHABE, M., AUDEBERT, C., DURAND-JOLY, I., BOLDRON, A., PIN, I., COGNET, O., PELLOUX, H., PREVOTAT, A., WALLAERT, B., WIZLA, N., THUMERELLE, C., TURCK, D. & THE MUCOFONG INVESTIGATION, G. 2020. Respiratory mycobiome and suggestion of inter-kingdom network during acute pulmonary exacerbation in cystic fibrosis. *Scientific Reports,* 10**,** 3589.

SUN, X., XIA, C., SUN, W. & SUN, S. 2025. Exploring Enterotype Characteristics of Chronic Kidney Disease Stages 3-5 Based on the Partitioning Around Medoids Clustering Algorithm. *Integrative Medicine in Nephrology and Andrology,* 12.

TERRANOVA, L., ORIANO, M., TERI, A., RUGGIERO, L., TAFURO, C., MARCHISIO, P., GRAMEGNA, A., CONTARINI, M., FRANCESCHI, E., SOTTOTETTI, S., CARIANI, L., BEVIVINO, A., CHALMERS, J. D., ALIBERTI, S. & BLASI, F. 2018. How to Process Sputum Samples and Extract Bacterial DNA for Microbiota Analysis. *Int J Mol Sci,* 19.

TUEFFERS, L., BARBOSA, C., BOBIS, I., SCHUBERT, S., HÖPPNER, M., RÜHLEMANN, M., FRANKE, A., ROSENSTIEL, P., FRIEDRICHS, A., KRENZ-WEINREICH, A., FICKENSCHER, H., BEWIG, B., SCHREIBER, S. & SCHULENBURG, H. 2019. Pseudomonas aeruginosa populations in the cystic fibrosis lung lose susceptibility to newly applied β-lactams within 3 days. *J Antimicrob Chemother,* 74**,** 2916-2925.

TUNNEY, M. M., EINARSSON, G. G., WEI, L., DRAIN, M., KLEM, E. R., CARDWELL, C., ENNIS, M., BOUCHER, R. C., WOLFGANG, M. C. & ELBORN, J. S. 2013. Lung microbiota and bacterial abundance in patients with bronchiectasis when clinically stable and during exacerbation. *Am J Respir Crit Care Med,* 187**,** 1118-26.

VALENTINI, T. D., LUCAS, S. K., BINDER, K. A., CAMERON, L. C., MOTL, J. A., DUNITZ, J. M. & HUNTER, R. C. 2020. Bioorthogonal non-canonical amino acid tagging reveals translationally active subpopulations of the cystic fibrosis lung microbiota. *Nature Communications,* 11**,** 2287.

VARGA, J. J., ZHAO, C. Y., DAVIS, J. D., HAO, Y., FARRELL, J. M., GURNEY, J. R., VOIT, E. & BROWN, S. P. 2022. Antibiotics Drive Expansion of Rare Pathogens in a Chronic Infection Microbiome Model. *mSphere,* 7**,** e00318-22.

VORONINA, O. L., RYZHOVA, N. N., KUNDA, M. S., LOSEVA, E. V., AKSENOVA, E. I., AMELINA, E. L., SHUMKOVA, G. L., SIMONOVA, O. I. & GINTSBURG, A. L. 2020. Characteristics of the Airway Microbiome of Cystic Fibrosis Patients. *Biochemistry (Mosc),* 85**,** 1-10.

WALDETOFT, K. W., SUNDIUS, S., KUSKE, R. & BROWN, S. P. 2022. Defining the Benefits of Antibiotic Resistance in Commensals and the Scope for Resistance Optimization. *mBio,* 14**,** e01349-22.

WEISER, R., RYE, P. D. & MAHENTHIRALINGAM, E. 2021. Implementation of microbiota analysis in clinical trials for cystic fibrosis lung infection: Experience from the OligoG phase 2b clinical trials. *Journal of Microbiological Methods,* 181**,** 106133.

WHELAN, F. J., HEIRALI, A. A., ROSSI, L., RABIN, H. R., PARKINS, M. D. & SURETTE, M. G. 2017. Longitudinal sampling of the lung microbiota in individuals with cystic fibrosis. *PLoS One,* 12**,** e0172811.

WIDDER, S., ZHAO, J., CARMODY, L. A., ZHANG, Q., KALIKIN, L. M., SCHLOSS, P. D. & LIPUMA, J. J. 2022. Association of bacterial community types, functional microbial processes and lung disease in cystic fibrosis airways. *Isme j,* 16**,** 905-914.

ZHAO, C. Y., HAO, Y., WANG, Y., VARGA, J. J., STECENKO, A. A., GOLDBERG, J. B. & BROWN, S. P. 2020. Microbiome data enhances predictive models of lung function in people with cystic fibrosis. *J Infect Dis.*

ZHAO, J., SCHLOSS, P. D., KALIKIN, L. M., CARMODY, L. A., FOSTER, B. K., PETROSINO, J. F., CAVALCOLI, J. D., VANDEVANTER, D. R., MURRAY, S., LI, J. Z., YOUNG, V. B. & LIPUMA, J. J. 2012. Decade-long bacterial community dynamics in cystic fibrosis airways. *Proc Natl Acad Sci U S A,* 109**,** 5809-14.